Metabolic trade-offs hide unforeseen benefits of plasmids carriage

Rafael C. Reding[1].

[1] Living Systems Institute, University of Exeter, Exeter EX4 4QD, UK.

Corresponding author: R.C.Reding-Roman@exeter.ac.uk.

Microbes can preserve plasmids in non-selective conditions, paying a metabolic cost—reduced growth rate—without getting any benefit from them. Explaining this paradox is challenging. Here I report that plasmids can change multiple traits simultaneously, making them unexpectedly beneficial. A competition between two identical *Escherichia coli* strains, S and R, where R bears a non-transmissible plasmid with a tetracycline-resistance gene, revealed that growth rate, biomass yield and lag are sensitive to plasmid carriage. Importantly these traits engaged in a trade-off that was previously unknown. R cells exploited it to preserve their plasmid and outgrow their plasmid-free counterpart S—with and without tetracycline. Most of the known plasmids are not transmissible, but they can replicate within their host. The above trade-off can explain the abundance of these plasmids in nature despite lacking horizontal transfer mechanisms.

Introduction

The 'plasmid paradox' (*1*) is founded on the seemingly contradictory abundance of plasmids among microbial communities. Plasmids are independent genetic elements that complement the chromosome of prokaryotes (*1*, *2*) and eukaryotes (*3*) alike. They can benefit cells harbouring them—notoriously in the form of resistance to antibiotics—but the metabolic costs associated with their upkeep reduce the host's growth rate (*1*, *4*). Clinicians and evolutionary biologists exploit the sensitivity of growth rate to plasmid carriage, using pairwise competition experiments to estimate the costs of plasmid maintenance (*5–9*). Their conclusion is straightforward: microbes without plasmids multiply faster in environments where plasmids are not beneficial, and overthrow microbes harbouring them (*4*, *8*). Bacteria, however, can preserve plasmids that have no evident benefit (*10–12*). Whence the paradox.

Some plasmids can spread horizontally (i.e. conjugation) and escape this paradox (*13*), the problem is that most of the known plasmids are unable to do just that (*14*). The metabolic alterations that plasmids introduce in their hosts are unclear (*5*, *15–17*), so I asked whether growth rate is the only life-history trait sensitive to plasmid carriage. It is not. I analysed the growth dynamics of two identical constructs (*18*) of *Escherichia coli*, one of which (R in the remainder) harbours a non-transmissible plasmid with a tetracycline resistance gene, and found that plasmids can also delay the onset of growth (lag) and increment biomass yield. Importantly, growth rate, lag, and yield engaged in a trade-off that was previously unknown.

Without tetracycline R exploited the trade-off in pairwise competition experiments that favoured yield over growth rate, preserving the plasmid while outgrowing S for 80< genera-

tions. During that time R maintained the plasmid without variations in the number of copies, but with tetracycline this number changed. Despite using concentrations below 2% the minimum inhibitory concentration, to allow the growth of the construct S, R-cells exposed to more antibiotic hosted more plasmids. The gain was detectable within 24h, and exposed the dependence of the aforementioned benefits on plasmid copy number. Mutants harbouring more plasmids had lower yields and shorter lags, consistently with the above trade-off, but their growth rate remained unchanged. This suggests that growth rate assumes the costs of plasmid acquisition, whereas other traits—yield and lag—assume those of hosting different copies. Thus, plasmids can be either costly or beneficial depending on which trait is under selective pressure.

Results

Plasmid-mediated trade-off between rate, yield and lag. Growth curves can provide insight into metabolic changes in bacteria. The transition from efficient to inefficient pathways, for example, can be detected analysing them (*19*, *20*). I therefore sought changes in the growth curves (see Methods) of two strains of *Escherichia coli* MC4100, one of which, R, bears the plasmid pGW155B (*18*). This plasmid contains a tetracycline resistance gene, *tet(36)*, and is non-transmissible, that is, it cannot be transferred horizontally to other cells. Now, the growth curves showed that harbouring pGW155B penalised the growth rate of R by 29.41% ± 2.57% (mean ± standard error, Mann-Whitney U-test $p < 0.001$) compared to its sensitive counterpart, S, as we may expect (Figure 1A). But they also exposed noteworthy differences in other growth parameters.

Despite their lower growth rate, cells harbouring pGW155B attained larger population sizes than cells without it. I used this parameter to estimate the biomass yield (y) of both strains, a proxy for metabolic efficiency (*20*) defined as $y = K/glc$, where K is the population size in the equilibrium or *carrying capacity* and glc the supply of glucose. This metric suggests that R cells, despite their slower growth rate, were the most efficient of both types (Mann-Whitney U-test for differences in carrying capacity $p \approx 0.021$, Figures 1B and C). Another parameter that I found sensitive to pGW155B was the lag phase—the period where cells negotiate their transition into growth—and its duration was considerably longer in R cells (Figure 1B, Mann-Whitney U-test $p < 0.001$). In other words, growth rate, yield and lag engage in a trade-off that was previously unknown and that, in our experimental setting, is triggered by the acquisition of pGW155B.

Rate-yield-lag (RYL) trade-off changes the interpretation of carriage costs. Now, clinicians and evolutionary biologists measure drug sensitivity using different traits. The former frequently measure changes in bacterial density across a range of antibiotic concentrations (*21–24*), whereas the latter measure changes in growth rate (*7*, *9*, *25*). I therefore asked how the above trade-off influence the interpretation of antibiotic sensitivity tests, and exposed the strains S and R to a range of tetracycline concentrations to measure the minimum inhibitory concentration (MIC)—a metric of drug sensitivity commonly used in drug therapy design (*26*, *27*). The plasmid borne by R increased its resistance to tetracycline by $\sim 3,000\%$ irrespectively

of the trait I measured (Mann-Whitney U-test $p = 0.083$, ranksum $= 55$), but the MIC reported was, indeed, different for each trait (Figures 2A and S1A). Using growth rate data, the minimum inhibitory concentration for R was 8.343 ± 0.288 µg/mL of tetracycline (mean $\pm$ 95% confidence, Figure 2A), whereas using bacterial density data the MIC was 6.106 ± 0.272 µg/mL (Figure S1A). That is a $\sim$ 35% difference in the estimation of the same parameter. I found a similar gap for the tetracycline-sensitive strain S.

Importantly, whether pGW155B incurs in metabolic costs depends on which trait I measured. Growth rate and lag data suggests the plasmid is, indeed, costly to maintain (Figures 2A and S1B) but culture density data shows the opposite: harbouring pGW155B provides a benefit that helped R cells reach larger population sizes than their plasmid-free counterpart (Figures S1A). The trade-off between growth rate, yield and lag, triggered by pGW155B, explains this discrepancy.

Plasmid maintenance depends on the trait under selection. Growth rate is often used in microbiology as a proxy for microbial fitness (*1*, *8*, *9*) and, as I showed in Figure 1B, harbouring pGW155B imposed a reduction in growth rate in the construct R. Prior literature (*8*) showed that costly plasmids are purged from bacterial populations at an exponential rate very rapidly, so it is reasonable to assume that the construct S—without pGW155B—will outgrow R in sustained pairwise competitions. But given the RYL trade-off, it is no longer trivial to estimate the costs and consequences of plasmid carriage.

I tracked the growth rate of each construct grown in mixed cultures, with a 1:1 proportion, that were exposed to a range of tetracycline concentrations for five consecutive 24h seasons. Importantly I propagated the cultures once R reached the equilibrium (see Methods), thus, favouring yield over growth rate. Without antibiotic, the difference in growth rate between both constructs was negligible throughout the 5-day competition (Kruskal-Wallis H-test $p = 0.7840$, χ^2-statistic $= 1.7368$, Figure 2A). Growth data, however, shows that R outgrew S in every season (Figure 2B). This had unforeseen consequences.

The mutant selection window (*7*) is a theoretical framework to estimate drug concentration that are likely to select for drug-resistant mutants. Crucially, it relies on costs of resistance imposed by either chromosomal mutations or plasmids that protect against antimicrobials that, analog to those of plasmid carriage, reduce the growth rate of emerging resistant microbes. A key parameter of this framework is the minimal selective concentration or MSC (*7*). This concentration defines an boundary whereby resistant mutants have higher growth rates than their sensitive counterparts—inhibited by the drug—above the MSC, whereas below this concentration sensitive cells are the ones with higher growth rates. In other words, drug concentrations above the MSC select for resistant mutants whereas lower concentrations select for sensitive cells (*7*). Now, I estimated the MSC at 0.052 ± 0.004 µg/mL of tetracycline (Figure 2C). The MSC remained unchanged in mixed culture conditions (Kruskal-Wallis H-test $p \sim 0.1$, χ^2-statistic $= 7.6860$, Figure 2D) but, as Figure 2A showed, there is no clear selection for neither construct.

Given the above RYL trade-off I failed to detect MSCs using growth data. The selection coefficient (*28*) shows there was, indeed, selection for the strain R (Figure 2D) that is not

captured by metrics that rely on growth rate. Thus, as Figure 2B illustrates, the construct R—with pGW155B—can sustainably outgrow S—without pGW155B—despite growing at a slower rates, with and without antibiotic.

R-mutants with additional copies of pGW155B show phenotypic changes consistent with the RYL trade-off. During the 5-day competition the growth rate of R did not change, as we may expect given the low tetracycline concentrations I used (Welsch's $t-$test, $t-$statistic = 1.309, $p \approx 0.195$, and slope 95% confidence interval = (-0.178, 0.853), Figure 3A). However, the selection coefficient for this construct was positive. Further analysis of the 5-day phenotypic dataset revealed changed in lag and yield that are consistent with the RYL trade-off, namely, a reduction in lag is followed by a reduction in biomass yield (Figure 3B and C). Crucially, R cells exposed to more tetracycline showed lower yield and shorted lag, so I asked whether the number of plasmid borne by R cells changed through time. And it did.

To quantify the relative abundance of pGW155B within R cells, I sampled the mixed cultures on days one and five, calculated the proportion of chromosomal DNA corresponding to the construct R, and used quantitative polymerase chain reaction (qPRC) to measure the number of plasmids borne per cell (see Methods). The initial pool of cells from this strain, grown overnight and used to inoculate the cultures, contained 30.21 ± 6.72 copies of pGW155B per cell (mean ± 95% confidence). Without tetracycline, this number did not change significantly after one and five days of competition against S (Mann-Whitney U-test $p = 0.1$, ranksum = 15, Figure 3D). But the relative abundance of pGW155B changed rapidly with increasing drug concentrations. Within 24h the gain in plasmids was 2-fold, increasing 6- to 10-fold after five days of competition depending on tetracycline concentration (Figures 3E and F). Note that the highest concentration I used, 0.14 µ mg/mL, represents ∼1% the minimum inhibitory concentration for the construct R (see Methods).

To understand the relationship between plasmid copy number and drug concentration I fitted two mathematical models to qPCR data. First the linear model $p_c = p_0 + d\kappa$ and then the constant model $p_c = \kappa$, where κ denotes the slope or proportionality constant, p_0 the initial number of copies borne by each R cell and d the antibiotic supplied. The constant model, that assumes no change in the number of plasmids borne per cell, was extremely unlikely (relative likelihood $\approx 6.80\times10^{-42}$, Figure 3B). Instead the linear model suggests that plasmid copy number correlates with drug concentration, where the constant of proportionality $\kappa = 161.87 \pm 110.37$ plasmids per mL per microgram of drug per cell (t-statistic = 2.8745, $p = 0.0088$ and 95% confidence interval (51.5, 272.2)). Albeit significant, with an adjusted coefficient of determination (R^2) of 0.245, the linear model does not entirely capture the dynamics of qPCR data. A switch-like, non-linear model, say, the logistic model (see Methods), explained better the variation in the number of pGW155B that I observed (adjusted R^2 of 0.477). After five days of exposure to tetracycline the constant κ increased from 161.87 ± 110.37 to 880.19 ± 705.71 plasmids per mL per microgram of drug per cell (Figure 3C, t-statistic = 2.4446, $p = 0.0229$, and 95% confidence interval (174.5, 1585.9)). The predictive power declined for the logistic model, albeit it was still better than that for the linear model (adjusted $R^2 = 0.394$ *versus* 0.261).

Discussion

Plasmids are often portrayed as molecular parasites (*6*, *29*) that must *jump* between hosts to persist within a population or else, face extinction (*14*, *30*, *31*). Non-transmissible plasmids are an evolutionary anomaly that should not exist—specially if they transport genes that bear no benefit to their hosts. And yet, they represent the most common type of plasmid (*14*). The RYL trade-off helps explain their existence given that merely hosting a plasmid can be beneficial and, complementing prior research (*13*) on transmissible plasmids, explain the 'plasmid paradox'. Which begs the question whether it was a paradox to begin with. Growth rate is used extensively as the sole predictor for plasmid carriage but, it turns out, it is not the only trait that changes by hosting plasmids. If all the traits sensitive to plasmid carriage pay a cost, then growth rate may well be a good predictor of plasmid maintenance. As good as any of the other traits. However, if they do not, and all or some of the traits engage in a trade-off, then predicting plasmid maintenance may not be as trivial.

My study also suggests that plasmids can be highly sensitive to selection, given the sharp increase in the number of pGW155B borne by the construct R. Plasmid DNA can be substantially higher than chromosomal DNA in bacteria (*32*), and its relative abundance can change within the body during infections (*33*). It is therefore surprising that international AMR surveillance programmes (*34*) track only whether pathogens harbour plasmids. This has practical implications. For example, the curation of plasmids from bacteria *in vivo* is gaining momentum as an alternative to treat drug-resistant infections (*35–38*). But the technique is still inefficient. It should be self-evident that pathogens carrying fewer plasmids will be easier to treat than those bearing more copies of them, but the variations in the number of plasmids borne is often overlooked. Equally, in the case of antimicrobial resistance, microbes hosting more plasmids with antimicrobial-resistance genes should be less sensitive to antibiotics than those harbouring fewer plasmids. The plasmid might well be the same, just in different number. Reporting this information will be an asset in our fight against antimicrobial-resistant microbes.

Methods

Media and Strains. I used the strains of *Escherichia coli* GB(c) and Wyl (*39*) (a gift from Remy Chait and Roy Kishony), and M9 minimal media supplemented with 0.4% glucose and 0.1% casamino acids. I made tetracycline stock solutions from powder stock (Duchefa #0150.0025) at 5mg/mL in deionised water. Subsequent dilutions were made from this stock and kept at 4^oC.

Batch transfer protocol. I inoculated a 96-well microtitre plate containing 150µg/mL of media supplemented with tetracycline with a mixture of two overnight cultures, one of *E. coli* GB(c) and another of *E. coli* Wyl. The overnight culture for GB(c) was supplemented with 100ng/mL of tetracycline to preserve the plasmid pGW155B carrying *tet(36)* (*39*), and inoculated the microtitre plate with a mixture of the aforementioned overnight cultures, using different volumes so that the proportion between GB(c) and Wyl was 1:1 (Figure S2). I incubated the microtitre plate at 30^oC in a commercial spectrophotometer and measured the optical density

of each well at 600nm (OD_{600}), yellow florescence for the S strain (YFP excitation at 505nm, emission at 540nm), and cyan fluorescence for the R strain (CFP at 430nm/480nm) every 20min for 24h (a.k.a. *season*). After each season I transferred 1.5µL of each well, using a 96-well pin replicator, into a new microtitre plate containing fresh growth medium and tetracycline.

Growth parameter estimation. Fluorescence protein genes were constitutively expressed with an approximately constant fluorescence to optical density ratio (Figure S3). This enabled me to use fluorescence as a proxy for culture density in mixed culture conditions. I normalised fluorescence readings with respect to optical density readings using the ratio optical density to fluorescence in pure culture conditions as a reference.

I imported the resulting OD time series data set (Figures S4 and S5) into `MATLAB R2014b` to subtract background and calculate growth rate *per capita* (fitness, f) using the following algorithm. First, I fitted three mathematical models to data: 1) linear model $g(t) = b + f \cdot t$, 2) exponential model $g(t) = b + C \cdot \exp(f \cdot t)$ and 3) logistic model $g(t) = b + K/(1 + C \cdot \exp(-f \cdot t))$. The terms $g(t)$ denote culture growth through time (in OD, YFP, or CFP units), b the inoculum size used to subtract the background, C is a parameter and K the maximal population size attained. I used the fitness reported by the model with the lowest corrected Akaike Information Criterion (AICc).

Finally, I calculated the selection coefficient for the plasmid-harbouring strain using the regression model (*28*) $s = ln[R(t)/R(0)] \cdot t^{-1}$, where $R(0)$ is the initial ratio of resistant to susceptible (1:1) and $R(t)$ the ratio at time t.

Drug sensitivity parameter estimation. I defined the minimum inhibitory concentration (MIC) for each trait as the tetracycline required to reduce the trait of the bacterium by a factor of 99%, compared to the tetracycline-free control. The MICs were 0.364 ± 0.012 (mean ± 95% confidence), 0.351 ± 0.013 and 0.451 ± 0.019 µg/mL of tetracycline for the strain S using culture density, growth rate, and Malthusian growth respectively. For the strain R they were 11.121 ± 1.734, 9.103 ± 0.379, and 4.282 ± 0.038 µg/mL. Given the suppression of S in competition (Figure S6), I failed to detect its MICs in these conditions. I therefore relaxed the degree of inhibition from 99% to 90% (IC_{90}) to allow the estimation of drug sensitivity parameters in competition.

DNA material extraction. For each concentration, I sampled three representative 150µg/mL cultures that I divided into two groups for chromosome and plasmid DNA extraction. I ThermoScientific GeneJet DNA (#K0729) and GeneJet Plasmid (#K0502) extraction kits to extract chromosome and plasmid DNA from the samples, respectively, and used Qubit to quantify the yields. Both extracts were diluted accordingly in extraction buffer to normalise DNA across samples.

Quantitative PCR and plasmid copy number estimation. I used `primer3` to design two pairs of primers with melting temperature (T_m) of 60^oC and non-overlapping probes with T_m

of 70^{o}C. The amplicon ranges between 100 to 141bp depending on the locus (Table S1). Two reaction mixes were prepared using the kit 'Luminaris Color Probe Low ROX' (ThermoScientific #K0342), adding 0.3µM of each primer and 0.2µM of the probe as per manufacturer specifications. Following a calibration curve for each reaction (Figure S7) I added 0.01ng of chromosomal or plasmid DNA material to each of the reaction mixes.

To estimate the relative copies of pGW155B per R cell, I calculated the corresponding proportion of chromosomal DNA corresponding to the R-type from data in Figure 2D and used the formula (*8*)

$$cn = \frac{(1+E_c)^{Ctc}}{(1+E_p)^{Ctp}} \times \frac{S_c}{S_p},$$

where cn is the number of plasmid copies per chromosome, S_c and S_p are the size of the chromosome and pGW155B amplicon in bp, E_c and E_p the efficiency of the qPCR taken from data in Figure S7, and Ctc and Ctp are the cycles at which I first detected product amplification (C_t).

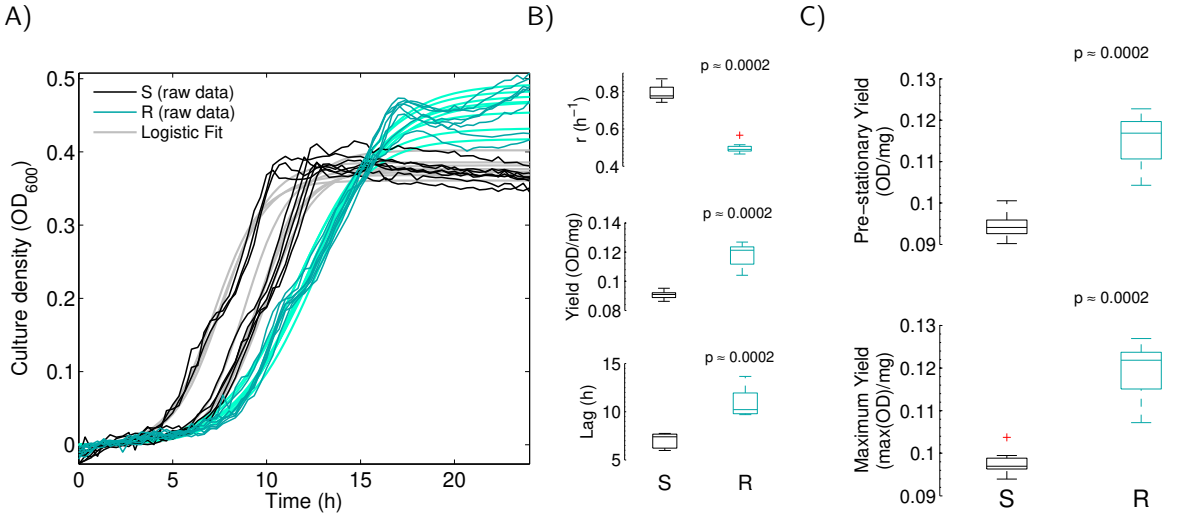

FIGURE 1. Rate-yield-lag (RYL) trade-off in strain carrying pGW155B. A) Overlapped growth curves of strains S (black) and R (cyan) in the absence of tetracycline. I estimated the growth rate (r), population size in the equilibrium (K), biomass yield (see main text), and lag from logistic models fitted to data (see Methods) shown in grey and light cyan, respectively. **B)** Box plots for each trait showing the median (centre of the box), 25th and 75th percentile of the data set. The whiskers extend to the most extreme data points that are not outliers, and these are individually represented. The p value shown on top of each box plot refers to a Mann-Whitney U-test that I used to test differences in the parameters between both strains. **C)** Alternative metrics for biomass yield (see Methods) using culture density at the onset of stationary phase (top) and maximal culture density at any given time. The p values correspond to Mann-Whitney U-tests.

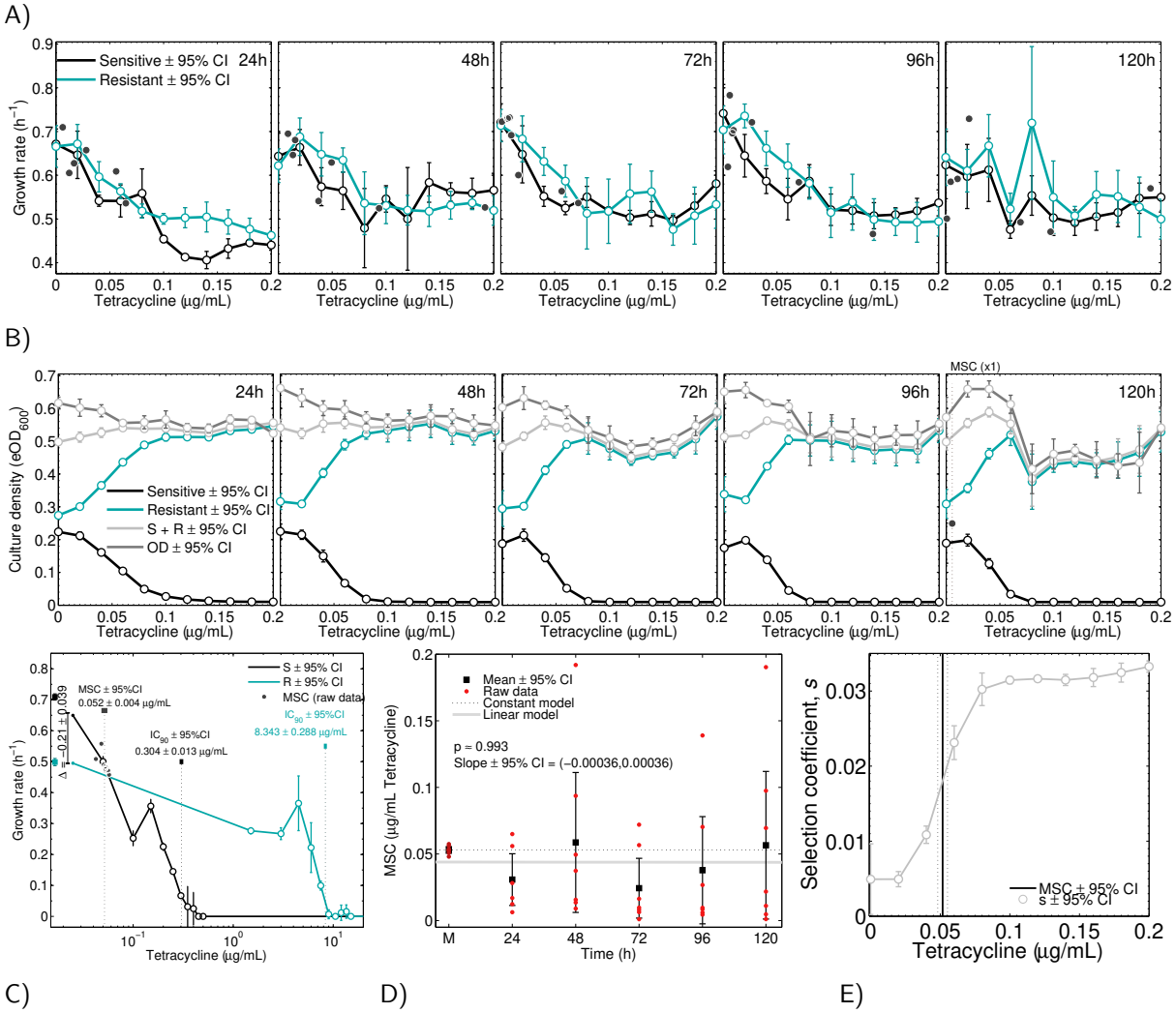

Figure 2. Growth rate alone is unable to capture plasmid maintenance. A) Change in *per capita* growth rate during the 5-day pairwise competition showing both sensitive (S, black) and resistant (R, cyan) *Escherichia coli* strains. In each subplot I present the mean growth rate ± 95% confidence across all tetracycline concentration corresponding to five consequence 24h seasons. The crossing point for each replicate—minimal selective concentration or MSC—is shown as small, black circles. **B)** Same as A), but I show change in cell density in optical density units derived from normalised fluorescence data (see Methods). In light grey I show the optical density of the mixed culture estimated from normalised fluorescence data, and in dark grey the optical density measured at 600nm **C)** Dose-response profile for each strain showing the change in growth rate with increasing tetracycline concentrations. I measured the costs of carrying pGW155B using growth rate from relative fluorescence growth data, with a decrease of 0.21 ± 0.039 h^{-1} for R (mean ± 95% confidence). The profiles of both strains crossed-over with 0.052 ± 0.004 µg/mL of tetracycline, defining the *minimal selective concentration*. **D)** Change in MSC over time with respect that measured in monoculture (M). Mean and 95% confidence interval are shown as black errorbars and the raw data as red dots. I fitted this data set to a constant (dotted line) and linear (light grey) models, the p value and slope shown correspond to the linear model. **E)** Selection coefficient for the resistant strain, s, at different tetracycline concentrations. I also represented the MSC in C) and its 95% confidence interval as a reference.

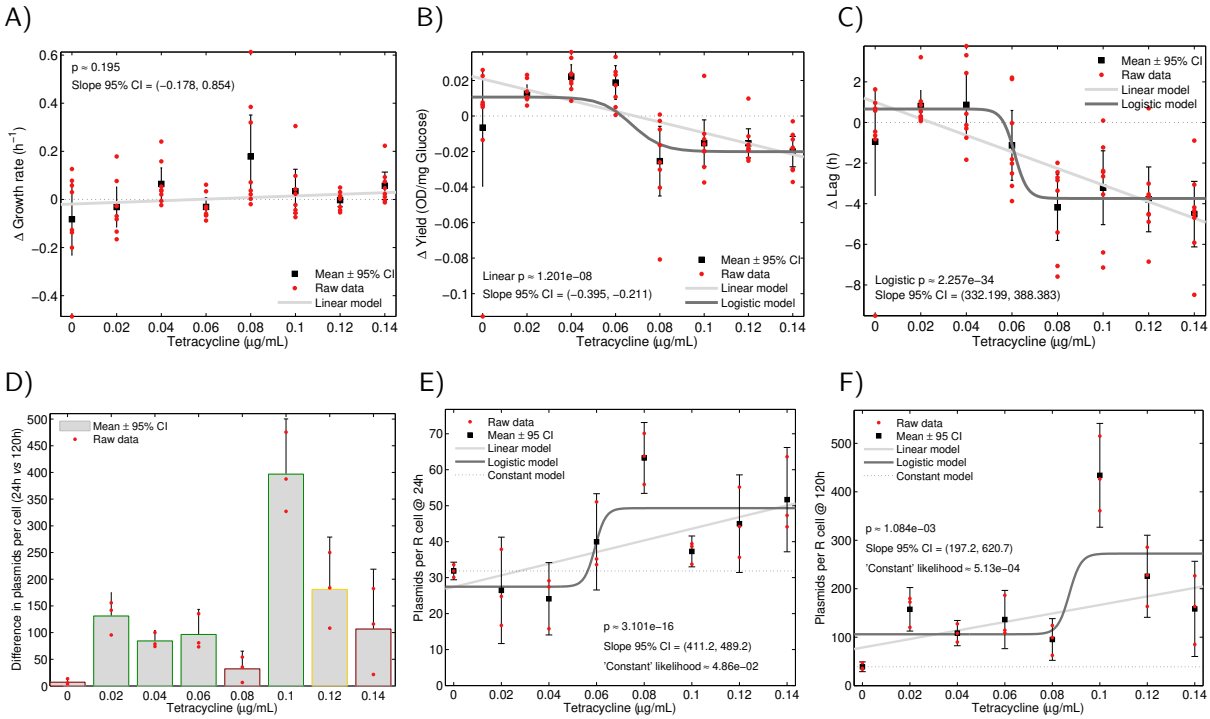

FIGURE 3. Variations in plasmid copy number induce phenotypic changes that are consistent with the RYL trade-off. A-C) Variation in growth rate (A), biomass yield (B), and lag (C) after 120h exposure to different tetracycline concentrations. I show mean and 95% confidence interval as black error bars and raw data in red dots. The dotted black line represents a constant model (a.k.a. no change), light grey line represents a linear model, and dark grey a logistic model. The statistics shown in A-C are those for the model with the highest adjusted coefficient of determination (R^2). **D)** Increment in pGW155B copy number after five days (120h) of exposure to tetracycline. Bars denote the mean and the errorbar 95% confidence of the mean; those with a green edge have a significant increase in copy number ($p < 0.05$) according to Welch's t-test, red if it was not ($p > 0.05$), and yellow if the test was inconclusive ($p \approx 0.05$). Raw difference in qPCR data is shown as red dots. **E-F)** Effect of tetracycline concentration on the number of plasmids borne by R cells after 24h (E) and 120h (F) of exposure to tetracycline. I show the mean and 95% confidence interval of qPCR data as black errorbars, and raw qPCR data as red dots. The black dotted line represents the prediction from the constant model, in light grey that for the linear model, and in dark grey the prediction for the logistic model. Statistical significance (p) for the slope parameter and confidence interval is shown for the model with highest adjusted coefficient of determination (R^2), which was the logistic in both data sets: 0.245 *versus* 0.477 for 24h data (linear *versus* logistic), and 0.261 *versus* 0.394 for 120h data. The likelihood function deemed the constant model unlikely (probability of 0.0486 for 24h data, 0.0005 for 120h data), so I did not consider its R^2.

References

1. Harrison, E. & Brockhurst, M. A. Plasmid-mediated horizontal gene transfer is a coevolutionary process. *Trends Microbiol.* **20,** 262–267 (2012).
2. Slater, F. R., Bailey, M. J., Tett, A. J. & Turner, S. L. Progress towards understanding the fate of plasmids in bacterial communities. *FEMS Microbiol. Ecol.* **66,** 3–13 (2008).
3. Esser, K., Kück, U., *et al. Plasmids of Eukaryotes: Fundamentals and Applications* ISBN: 9783642825859 (Springer Berlin Heidelberg, 2012).
4. Starikova, I., Sørum, V., *et al.* Fitness costs of various mobile genetic elements in Enterococcus faecium and Enterococcus faecalis. *J. Antimicrob. Chemother.* **68,** 2755–2765 (2013).
5. Rhee, J. I., Ricci, J. C. D., Bode, J. & Schügerl, K. Metabolic enhancement due to plasmid maintenance. *Biotechnol. Lett.* **16,** 881–884 (1994).
6. Bergstrom, C. T., Lipsitch, M. & Levin, B. R. Natural selection, infectious transfer and the existence conditions for bacterial plasmids. *Genetics* **155,** 1505–1519 (2000).
7. Gullberg, E., Cao, S., *et al.* Selection of resistant bacteria at very low antibiotic concentrations. *PLoS Pathog.* **7,** e1002158 (July 2011).
8. Millán, A. S., Peña-Miller, R., *et al.* Positive selection and compensatory adaptation interact to stabilize non-transmissible plasmids. *Nat. Commun.* **5** (2014).
9. Day, T., Huijben, S. & Read, A. F. Is selection relevant in the evolutionary emergence of drug resistance? *Trends Microbiol.* **23,** 126–133 (2015).
10. Sherratt, D. The Maintenance and Propagation of Plasmid Genes in Bacterial Populations The Sixth Fleming Lecture. *Microbiology* **128,** 655–661 (1982).
11. Byrd, J. J. & Colwell, R. R. Long-term survival and plasmid maintenance of Escherichia coli in marine microcosms. *FEMS Microbiol. Ecol.* **12,** 9–14 (1993).
12. Heuer, H, Krögerrecklenfort, E, *et al.* Gentamicin resistance genes in environmental bacteria: prevalence and transfer. *FEMS Microbiol. Ecol.* **42,** 289–302 (2002).
13. Lopatkin, A. J., Meredith, H. R., *et al.* Persistence and reversal of plasmid-mediated antibiotic resistance. *Nat. Commun.* **8,** 1689 (2017).
14. Smillie, C., Garcillán-Barcia, M. P., Francia, M. V., Rocha, E. P. & de la Cruz, F. Mobility of plasmids. *Microbiol. Mol. Biol. Rev.* **74,** 434–452 (2010).
15. Diaz Ricci, J. C. & Hernández, M. E. Plasmid effects on Escherichia coli metabolism. *Crit. Rev. Biotechnol.* **20,** 79–108 (2000).
16. Gonçalves, G. A., Bower, D. M., Prazeres, D. M., Monteiro, G. A. & Prather, K. L. Rational engineering of Escherichia coli strains for plasmid biopharmaceutical manufacturing. *Biotechnol. J.* **7,** 251–261 (2012).

17. Baltrus, D. A. Exploring the costs of horizontal gene transfer. *Trends Ecol. Evol.* **28,** 489–495 (2013).

18. Chait, R., Shrestha, S., Shah, A. K., Michel, J.-B. & Kishony, R. A Differential Drug Screen for Compounds That Select Against Antibiotic Resistance. *PLoS One* **5,** e15179 (2010).

19. Scott, M., Klumpp, S., Mateescu, E. M. & Hwa, T. Emergence of robust growth laws from optimal regulation of ribosome synthesis. *Mol. Syst. Biol.* **10,** 747 (2014).

20. Reding-Roman, C., Hewlett, M., *et al.* The unconstrained evolution of fast and efficient antibiotic-resistant bacterial genomes. *Nat. Ecol. Evol.* **1,** 0050 (2017).

21. Andrews, J. M. Determination of minimum inhibitory concentrations. *J. Antimicrob. Chemother.* **48,** 5–16 (2001).

22. Drlica, K. & Zhao, X. Mutant selection window hypothesis updated. *Clin. Infect. Dis.* **44,** 681–8 (Mar. 2007).

23. Andersson, D. I. & Hughes, D. Antibiotic resistance and its cost: is it possible to reverse resistance? *Nat. Revs. Microbiol.* **8,** 260–271 (2010).

24. Choi, J., Yoo, J., *et al.* A rapid antimicrobial susceptibility test based on single-cell morphological analysis. *Sci. Transl. Med.* **6,** 267ra174 (2014).

25. Rosenbloom, D. I., Hill, A. L., Rabi, S. A., Siliciano, R. F. & Nowak, M. A. Antiretroviral dynamics determines HIV evolution and predicts therapy outcome. *Nat. Med.* **18,** 1378–1385 (2012).

26. Finberg, R. W. & Guharoy, R. in *Clinical Use of Anti-infective Agents* 5–14 (Springer, 2012).

27. Ajmal, S., Saleh, O. A. & Beam, E. Development of high-grade daptomycin resistance in a patient being treated for Corynebacterium striatum infection. *Antimicrob. Agents. Chemother.* **61** (2017).

28. Dykhuizen, D. E. Experimental Studies of Natural Selection in Bacteria. *Annu. Rev. Ecol. Syst.* **21,** 373–398 (1990).

29. Svara, F. & Rankin, D. J. The evolution of plasmid-carried antibiotic resistance. *BMC Evol. Biol.* **11,** 130 (2011).

30. Subbiah, M., Top, E. M., Shah, D. H. & Call, D. R. Selection pressure required for long-term persistence of bla CMY-2-positive IncA/C plasmids. *Appl. Environ. Microbiol.* **77,** 4486–4493 (2011).

31. Carroll, A. C. & Wong, A. Plasmid persistence: costs, benefits, and the plasmid paradox. *Can. J. Microbiol.* **64,** 293–304 (2018).

32. Zhong, C., Peng, D., *et al.* Determination of plasmid copy number reveals the total plasmid DNA amount is greater than the chromosomal DNA amount in Bacillus thuringiensis YBT-1520. *PLoS One* **6,** e16025 (2011).

363 *33.* Wang, H., Avican, K., *et al.* Increased plasmid copy number is essential for Yersinia T3SS
364 function and virulence. *Science* **353,** 492–495 (2016).

365 *34.* *European Centre for Disease Prevention and Control. EU protocol for harmonised monitor-*
366 *ing of antimicrobial resistance in human Salmonella and Campylobacter isolates* tech. rep.
367 (2016).

368 *35.* Baquero, F., Coque, T. M. & de la Cruz, F. Eco-Evo drugs and strategies: the need for novel
369 tools to fight antibiotic resistance. *Antimicrob. Agents. Chemother.* AAC–00013 (2011).

370 *36.* Bikard, D., Euler, C. W., *et al.* Exploiting CRISPR-Cas nucleases to produce sequence-
371 specific antimicrobials. *Nat. Biotech.* **32,** 1146 (2014).

372 *37.* Kamruzzaman, M., Shoma, S., Thomas, C. M., Partridge, S. R. & Iredell, J. R. Plasmid
373 interference for curing antibiotic resistance plasmids in vivo. *PloS One* **12,** e0172913 (2017).

374 *38.* Buckner, M. M., Ciusa, M. L. & Piddock, L. J. Strategies to combat antimicrobial resistance:
375 anti-plasmid and plasmid curing. *FEMS Microbiol. Rev.* **42,** 781–804 (2018).

376 *39.* Chait, R., Craney, A & Kishony, R. Antibiotic interactions that select against resistance.
377 *Nature* **446,** 668–671 (2007).

378 **Acknowledgements:** I thank R. Beardmore for in-depth comments on the manuscript; and
379 members of the Beardmore and Gudelj laboratories for comments. **Competing interests:** The
380 author declares no competing interests.

Supplementary Tables

Table S1. Primers and probes designed using `Primer3`. Amplicon ranging from 100 to 141bp. T_m indicates the estimated melting temperature.

Target gen	Sequence ($5' \rightarrow 3'$)	T_m (^oC)	Feature
tatB	CGATGAAGCGTTCCTACGTT	60.27	Forward
	TCATGCGCAGCTTCATTATC	59.94	Reverse
	AAGGCGAGCGATGAAGCGCA	70.70	Probe
tet(36)	ATTGGGCATCTATTGGCTTG	59.22	Forward
	CCGATTCACAGGCTTTCTTG	60.76	Reverse
	AGCCTTTGCCAATTGGGGCG	70.37	Probe

Supplementary Figures

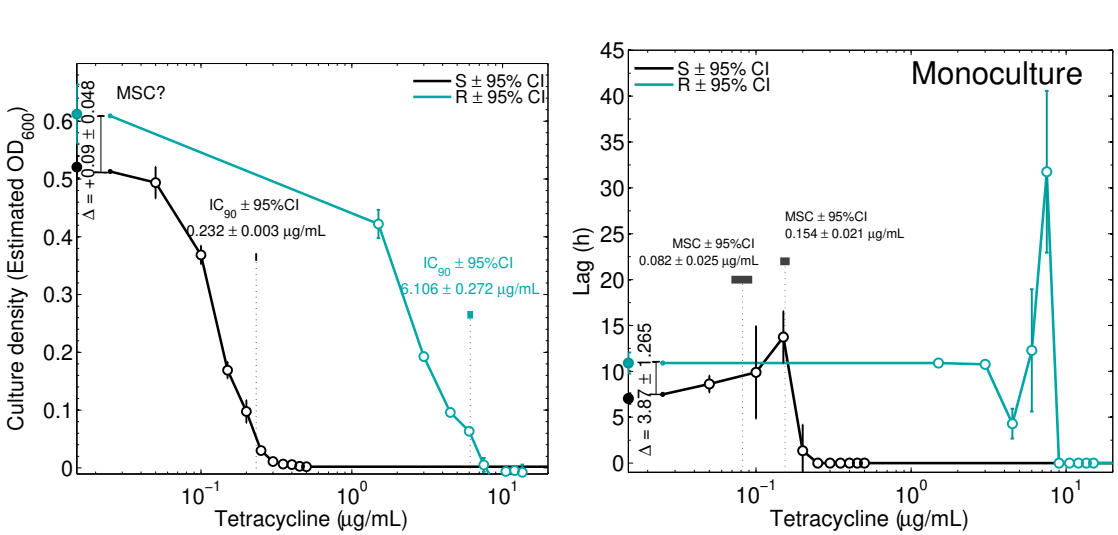

Figure S1. Dose-response profile for tetracycline using culture density and lag data. Dose-response profiles for each strain showing the change in culture density (A) and lag (B) with increasing tetracycline concentrations. The difference in R growth with respect to S was positive in antibiotic-free conditions (mean ± 95% confidence). Consequently, I could not detect any tetracycline concentration at which the profiles crossed over—*minimal selective concentration*—and establish the selection window for S. I estimated culture density from fluorescence data normalised with respect to optical density data (see Methods). In lag data, the difference between both types without tetracycline was negative and, thus, I could detect two MSCs at 0,082 ± 0.025 and .0.154 ± 0.021 µg/mL of tetracycline.

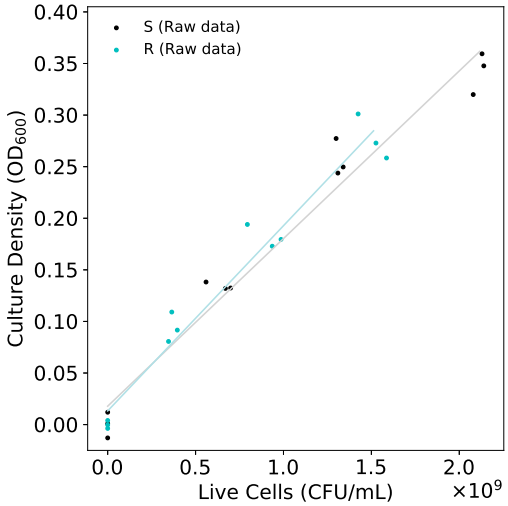

FIGURE S2. Calibration curve to translate optical density data to number of *Escherichia coli* cells. I fitted the linear model $a = bx + c$ to optical density and colony counting data (dots) to calculate the number of optical density units (OD_{600}) per cell. a denotes the optical density readings measured at 600nm, c the crossing point with the $y-$axis when $x = 0$, and b the conversion factor between optical density and number of cells (x). I interpolating optical density readings to calculate the number of cells within a culture as $x = (a - c)/b$. For the strain S, $b = 1.62 \times 10^{-}10\ OD \cdot mL \cdot CFU^{-1}$ and $c = 1.78 \times 10^{-2}\ OD$, whereas for R $b = 1.79 \times 10^{-10}\ OD \cdot mL \cdot CFU^{-1}$ and $c = 1.33 \times 10^{-2}\ OD$.

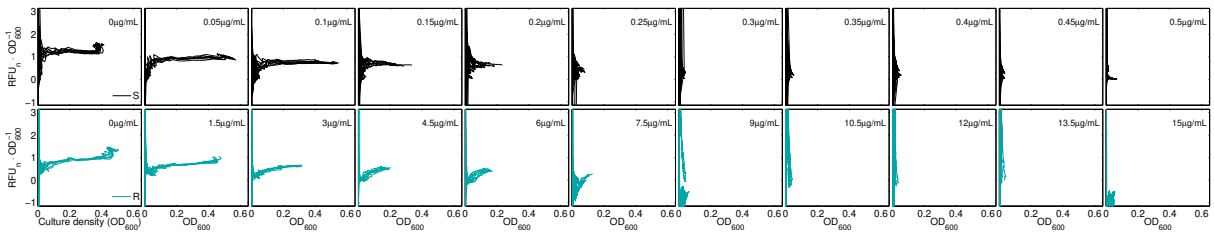

FIGURE S3. Changes in relative fluorescence over time in both R and S strains. Raw change in florescence, per optical density units, measured every 20min for 24h for the S- (black) and R-type. Each column represents the data set for each tetracycline concentration used.

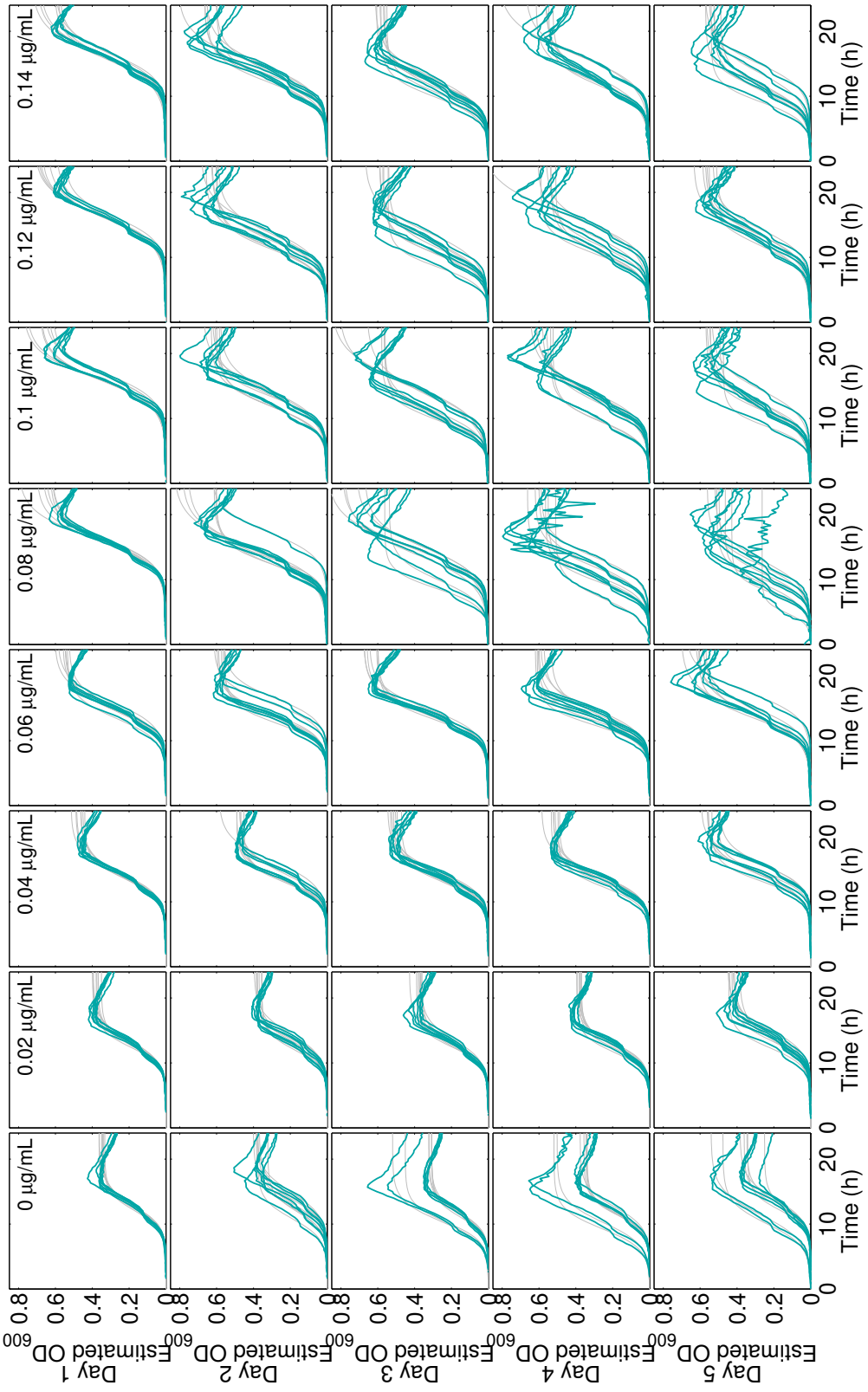

408 **Figure S4. Raw data and model fit for resistant R strain.** Raw optical Density data for GB(c)
409 measured every 20min for five 24h seasons (blue). The best fit to data (see Methods in main text) used
410 to calculate bacterial fitness is shown in grey. Each column represents the data set for one 24h season
412 and each row the data set for one tetracycline concentration.

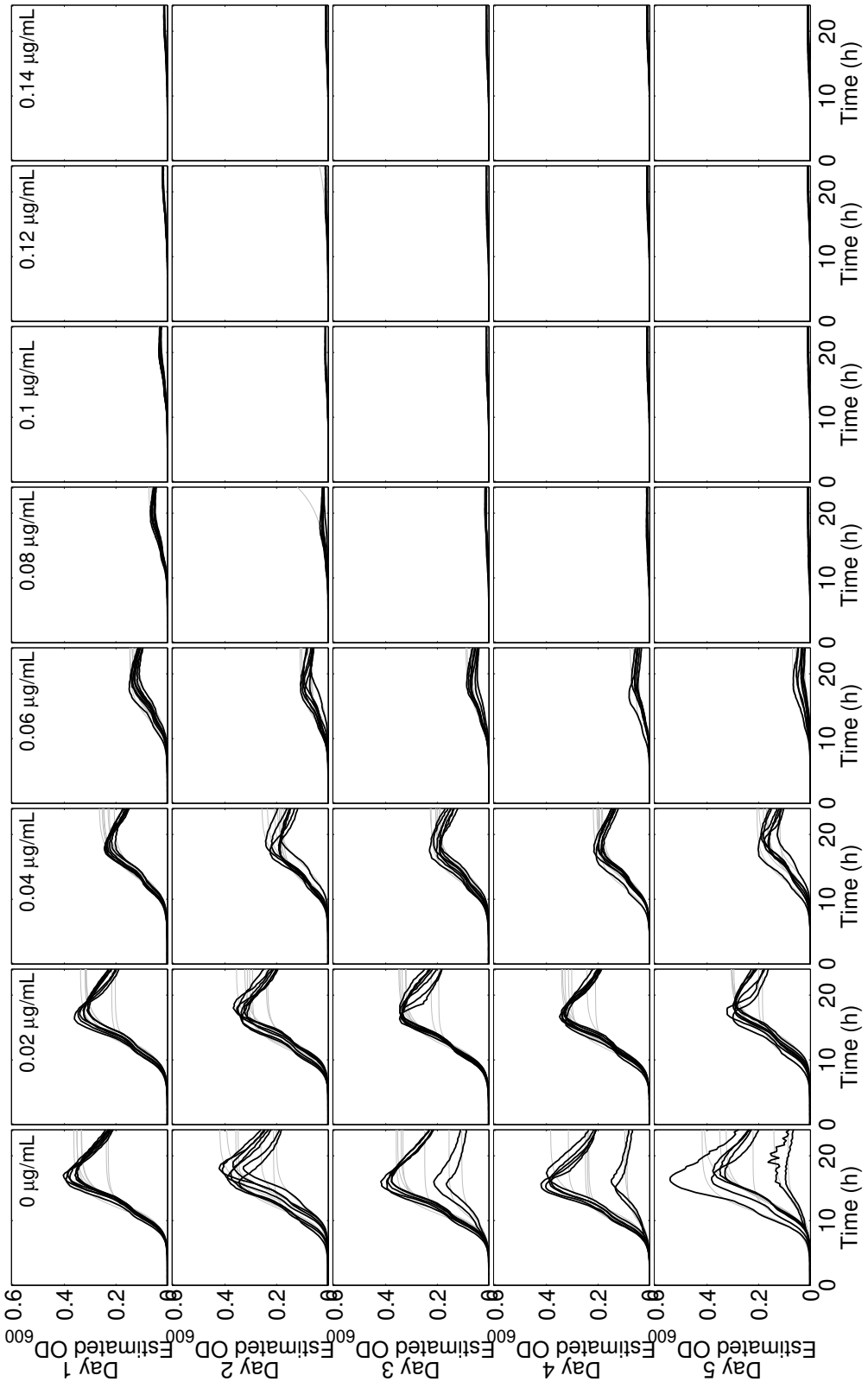

Figure S5. Raw data and model fit for sensitive S strain. Raw optical Density data for Wyl measured every 20min for five 24h seasons (black). The best fit to data (see Methods in main text) used to calculate bacterial fitness is shown in grey. Each column represents the data set for one 24h season and each row the data set for one tetracycline concentration.

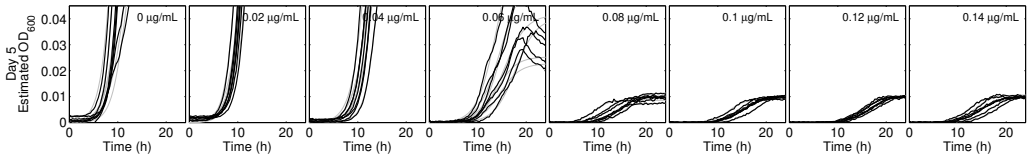

FIGURE S6. Sensitive type not fully outcompeted during the competition. Augmented detail of the evolved dose-response profiles of the tetracycline sensitive strain S after five days of exposure to tetracycline. Raw optical Density data measured every 20min for five 24h seasons (black). The best fit to data (see Methods in main text) used to calculate bacterial fitness is shown in grey. Each column represents the data set for one 24h season and each row the data set for one tetracycline concentration.

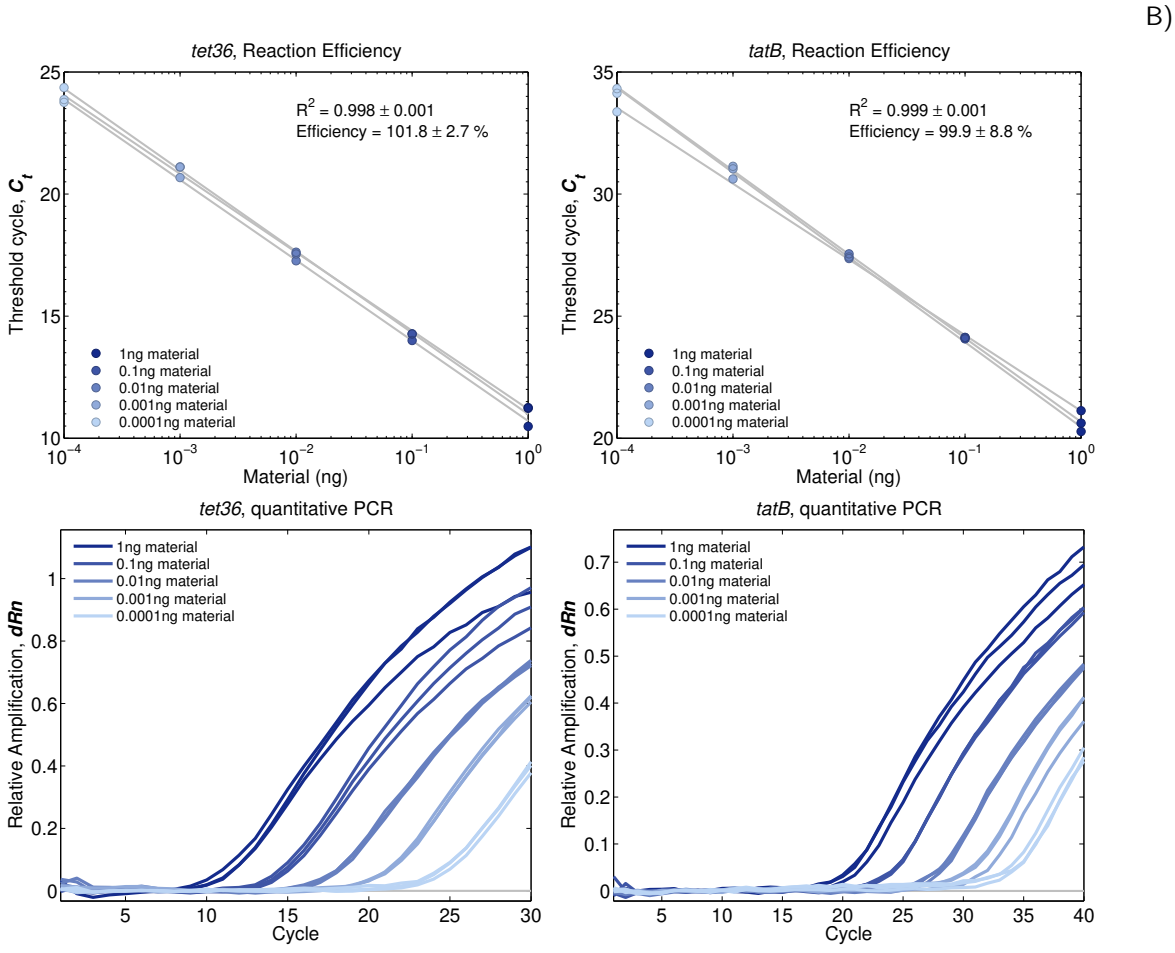

FIGURE S7. Quantitative PCR calibration curves for *tet(36)* and *tatB*. Reaction efficiency for the set of primers and probes listed in the 'methods' section for *tet(36)* (A) and *tatB*. The efficiency was calculated as $E_f = 10^{-1/Slope} - 1$, and the slope term calculated by fitting a linear model to qPCR threshold cycle (C_t) data. The mean ± standard deviation for the coefficient of determination R^2 and efficiency are shown in the figures. The amplification curves for each reaction are shown in C) and D), respectively.